17th World Conference on Earthquake Engineering, 17WCEE

Sendai, Japan - September 13th to 18th 2020

BEHAVIOR OF POORLY DETAILED RC FRAMES WITH LOW STRENGTH CONCRETE AND URM INFILL UNDER HIGH AXIAL LOADS

S. M. N. Adnan(1), Y. Fukutomi(2), Y. Haga(3), K. Matsukawa(4), Y. Nakano(5)

(1) *Graduate student, Graduate school of Eng., Department of Architecture, The University of Tokyo, nhdadnan@iis.u-tokyo.ac.jp*
(2) *Researcher, Kobori Research Complex, fukutomi@kobori-takken.co.jp*
(3) *Senior Collaborator, Institute of Industrial Science, The University of Tokyo, y-haga@iis.u-tokyo.ac.jp*
(4) *Research Associate, Institute of Industrial Science, The University of Tokyo, mtkw@iis.u-tokyo.ac.jp*
(5) *Professor, Institute of Industrial Science, The University of Tokyo, iisnak@iis.u-tokyo.ac.jp*

Abstract

In this study, the lateral cyclic static-load response of two 1/2.5 scale, 2-story, 2-bay RC frame specimens with low strength concrete and straight anchorage of beam longitudinal bars in the external beam-column joints under very high axial load are tested to address the condition of existing older buildings in Bangladesh. One of the specimens had unreinforced masonry (URM) infill walls in both stories of one bay, and the other specimen had no masonry infill walls (MIW). Significant differences in maximum strength and failure mechanisms were observed between the two specimens. The primary failure mechanism of the bare frame specimen (BF) involved the pullout of rebars from the external beam-column joints due to the straight anchorage and hinging of the columns at the bottom of 1st story and top of 2nd story. The specimen with masonry infill walls (BF+MIW) suffered column snap-through shear failure in the 1st story interior column and simultaneous sliding shear failure at the beam-wall interface of the 1st story. The BF and BF+MIW specimens showed maximum lateral strength of 4.02kN and 66.20kN, respectively. For both specimens, the strength of RC members was evaluated using the stress block assumptions and the Architectural Institute of Japan (AIJ) standard. The column snap-through shear strength and the sliding shear failure of the beam-wall interface were calculated using the Japan Building Disaster Prevention Association (JBDPA) standard and Mohr-Coulomb failure criterion, respectively. The estimated lateral strength for the specimen shows good agreement with the experimental results. Although the sudden collapse of frames might be expected due to the low strength of concrete and very high axial loads, the authors found that the presence of straight anchorage of beam longitudinal bars in the exterior beam-column joints in an RC frame will lead to pullout failure at the joints. For a weak RC frame structure with relatively stronger and stiffer masonry infill walls, the test results of the BF+MIW specimen demonstrate that failure mechanism involving the simultaneous snap-through shear failure of the columns and sliding shear failure at the beam-wall interfaces is a major possibility.

Keywords: low strength concrete; straight anchorage; high axial load; masonry infill wall; snap-through shear of column

1. Introduction

In the developing and under-developed countries around the world, numerous buildings can be found that are constructed without following proper guidelines, using low-quality construction materials, and lack proper seismic detailing. The issues regarding the design and construction of these buildings that may affect the seismic performance are often very diverse and may depend on individual building although some issues can be observed more frequently. The fact that makes the situation more distressing is that there is no clear trend that can be observed towards the correction of the inadequate construction practices that have been frequently detected, discussed, and published through the years. These buildings possess a potential risk of collapse in the event of an earthquake and therefore need seismic performance evaluation. For instance, if we look at the case of Bangladesh, which lies in a seismically active zone, recent surveys have found the existence of very low strength concrete (≤ 13.5MPa) in RC buildings [1–3]. Due to the existence of low strength concrete in the members, the columns are under a very high axial force ratio. Most of the buildings in the country that were constructed before the publication of its first building code "Bangladesh National Building Code (BNBC) 1993" [4] did not follow any proper guidelines of design and construction. Some features of these buildings are straight anchorage of beam longitudinal reinforcements and no transverse reinforcements in beam-column joints, 90° hooks in ties and stirrups, etc. Proper evaluation of the seismic performance these buildings are required for future retrofitting of these buildings.

To investigate the structural performance of such inappropriately designed and constructed buildings, two 1/2.5 scale 2-story 2-bay RC frames have been tested under high axial loads in the columns. Displacement controlled lateral loading is applied to the specimens. Brick masonry infill walls were added to one of the specimens in the right bay of both stories to understand how MIWs affect the behavior of RC frames with low strength concrete. In both specimens, beam longitudinal bars were inserted straight into the exterior beam-column joints to assess the effect of straight anchorage on the performance of RC frames.

This study presents the details of the experimental program and the evaluation of the results obtained from the RC frames tested. The lateral capacity of the specimens is evaluated using methods and guidelines suggested by the American Concrete Institute (ACI) [5], Architectural Institute of Japan (AIJ) [6] and Japan Building Disaster Prevention Association (JBDPA) [7] and based on observed failure mechanism. Finally, the calculated results are compared with the experimental results.

2. Experimental program

2.1 Prototype building and scaled specimen

Researches and surveys conducted previously have identified some common problems in RC buildings of Bangladesh that are presented in Table 1 [1–3]. Based on interviews of experts and professionals and considering the conditions 1, 7-10 and 12 listed in Table 1, a prototype building is assumed as shown in Fig. 1. The assumed prototype building is an example case of residential buildings found in Bangladesh, consisting of 6 stories, each story is 3m in height and the plan area of the building is 12m × 8m. The assumed prototype building has a concrete strength less than 10 MPa in the members, 250mm × 250mm column cross-section and high axial force ratio, η (= $N/f_c{}'bD$) in the columns (N = axial force, $f_c{}'$ = compressive strength of concrete, b = width of column, D = depth of column). It is to be noted that the minimum dimension of an RC member allowed by BNBC 1993 was 250mm [4]. The interior and exterior columns have the axial force ratio η_{int} = 0.84 and η_{ext} = 0.40, respectively. One span of the interior frame in the transverse direction as shown in Fig. 1, is selected to design the 2-story 2-bay 1/2.5 scale frame specimens. The specimens represent the bottom two stories of the prototype building. One of the RC frame specimens was constructed with no infills and to understand the effect of masonry infill walls on the seismic performance of RC frames, brick infill walls were added to the other RC frame in one bay of both stories with concrete members of identical design as the previous specimen. Henceforth, the bare frame specimen and the specimen with brick infill walls will be referred to as BF and BF+MIW, respectively.

Table 1 – Problems found in RC buildings in Bangladesh

No.	Problem	Specimen design
1.	**Low strength of concrete (≤ 13.5 MPa)**	**Less than 10 MPa**
2.	Unavailability of structural design drawings	
3.	Insufficient maintenance or repair	
4.	Weak cold joints in structural members	
5.	One-way slab system	
6.	Insufficient lap length of steel bars	
7.	**90° hooks in ties and stirrups**	**90° hooks**
8.	**High axial force ratio**	$\boldsymbol{\eta_{int}}$ **= 0.84,** $\boldsymbol{\eta_{ext}}$ **= 0.40**
9.	**Low or no transverse reinforcement in beam-column joints**	**No transverse reinforcement in the beam-column joints**
10.	**Neglect of MIW contribution**	**Rational assumption for MIW contribution**
11.	Narrow gap at expansion/structural joints	
12.	**Discrepancy between drawing and construction**	**Straight anchorage of beam reinforcement**

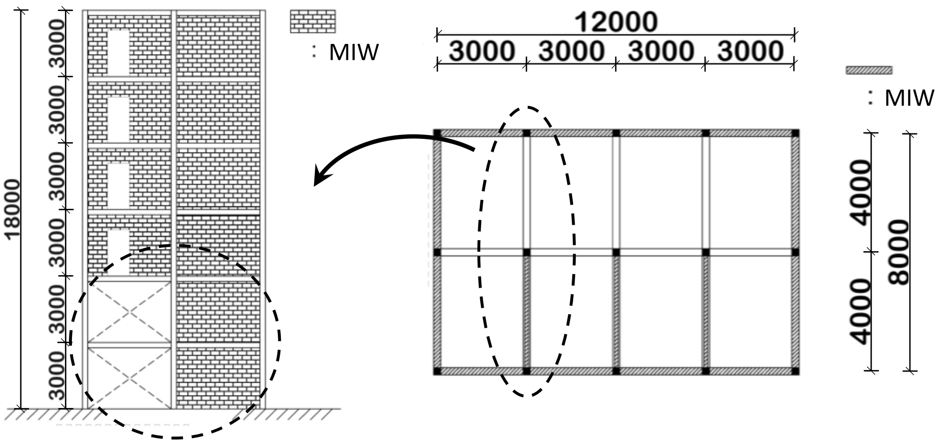

Fig. 1 – Assumed prototype building (unit: mm)

2.2 Design of scaled specimen

Fig. 2 and Fig. 3 show the design details of the 1/2.5 scale BF and BF+MIW specimens. The floor height is 1.2m and each of the spans is 1.6m. The cross-sections of the columns and the beams in the specimen are 100mm × 100mm and 130mm × 100mm respectively. A portion of the slab of 160mm width and 50mm thickness is cast monolithically on both sides of the beams. All the stirrups and ties in the specimens have 90° hooks and no transverse reinforcement was placed inside the beam-column joints. Straight anchorage of beam longitudinal bars inside the beam-column joints can be found in many buildings in Bangladesh. To address this condition in the specimens the beam longitudinal bars are inserted and continued straightly inside the columns as shown in Fig. 3. Table 2 shows the mechanical properties and design details of the concrete members of the specimens. To assess the pullout capacity of rebars in the straight anchorage, separate pullout tests were conducted under compressive forces applied perpendicular to the direction of the pullout force. The pullout test scheme is shown in Fig. 4.

The concrete was cast vertically in three stages. The casting sequence was as follows; at first, the base was cast, in the second stage concrete of 1st story was cast up to the 1st-floor beam and finally, concrete of 2nd story was cast up to the 2nd-floor beam. Between the casting stages, there was a one-week gap. The brick infill walls were added to the BF+MIW specimen after the removal of formwork. The cement/sand ratio of the mortar layer in the MIW was 1:4.

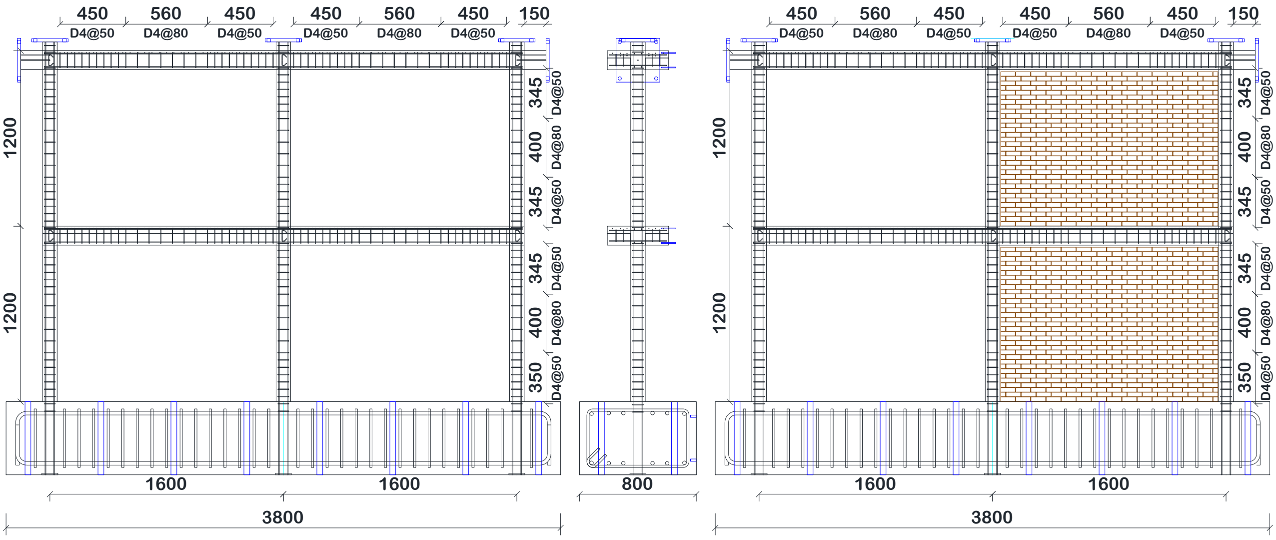

(a) BF specimen (b) BF+MIW specimen

Fig. 2 – 1/2.5 scale 2-story 2-bay frame specimens tested (unit: mm)

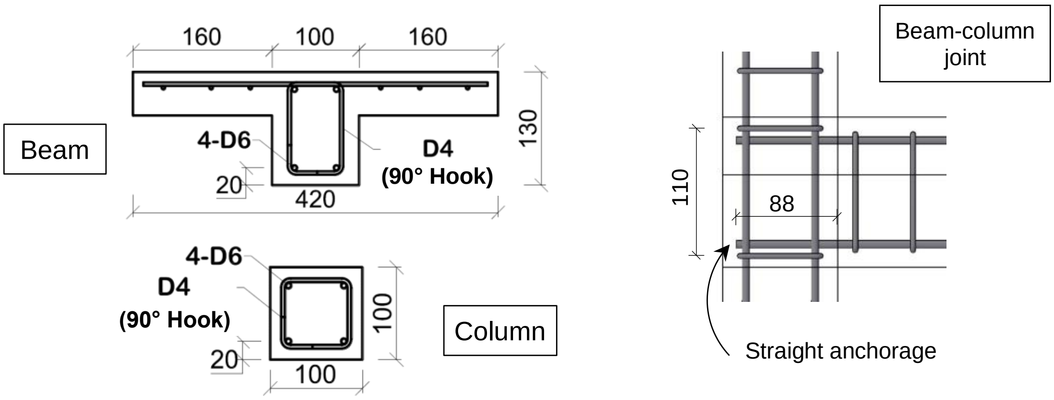

Fig. 3 – Details of the concrete members of the specimens (unit: mm)

2.3 Test program

Fig. 5 shows the lateral loading scheme applied to specimen which is controlled by the drift angle R. R is defined as the average of the lateral drifts at the center of each beam-column joint of the uppermost beam, Δ divided by the height from the bottom of the specimen to the center of the uppermost beam, h (= 2335mm). When the lateral load fell below 80% of the maximum lateral capacity the loading was terminated.

The loading system for the static cyclic in-plane loading applied to the specimens is shown in Fig. 6. The horizontal jacks were connected only to the ends of the uppermost beam. Vertical actuators were connected to the top of each column to apply a constant axial force in the columns. On top of the interior column, a constant axial force of 40.00kN (η_{int} = 0.84) and on top of the exterior columns a constant axial load of 18.76kN (η_{ext} = 0.40) were applied. Additionally, a distributed load of 1.6kN/m was applied to the beams considering a design dead load. To eliminate the out-of-plane response during the tests, two pantographs were used as shown in Fig. 6. More details of the experimental program can be found from reference [8–10].

Table 2 Material properties and specimen design

Material strength	Concrete strength	BF specimen	1F	4.74MPa
			2F	8.40MPa
		BF+MIW specimen	1F	5.22MPa
			2F	8.65MPa
	Steel bar (yield)			375MPa (SD295)
	Brick unit (compressive)			30.3MPa
	Mortar (cylinder compressive)			9.04MPa
	Masonry prism (compressive)			27.9MPa
	Pullout strength (BF Specimen)		1F	1.19kN
			2F	1.69kN
Dimensions	Floor height × Span			1,200mm × 1,600mm
	Column section (b×D)			100mm × 100 mm
	Beam section (b×D)			130mm × 100 mm
	Slab width			160mm
	Slab thickness			50mm
	Brick unit			100 mm × 46mm × 30mm
	Mortar layer thickness			2mm

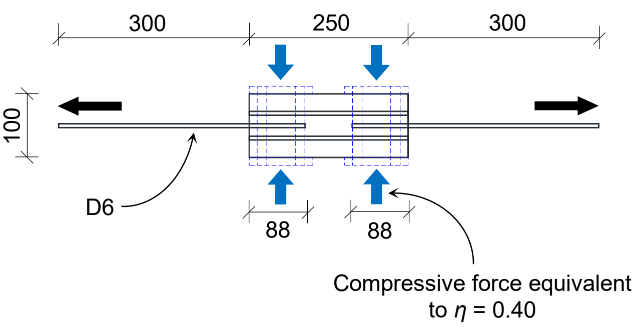

Fig. 4 – Rebar pullout test scheme under compression

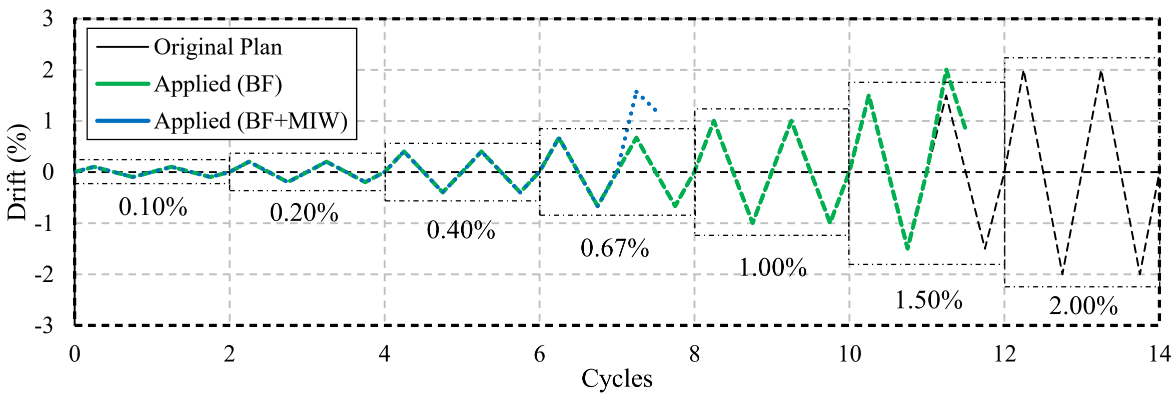

Fig. 5 – In-plane displacement controlled lateral loading scheme

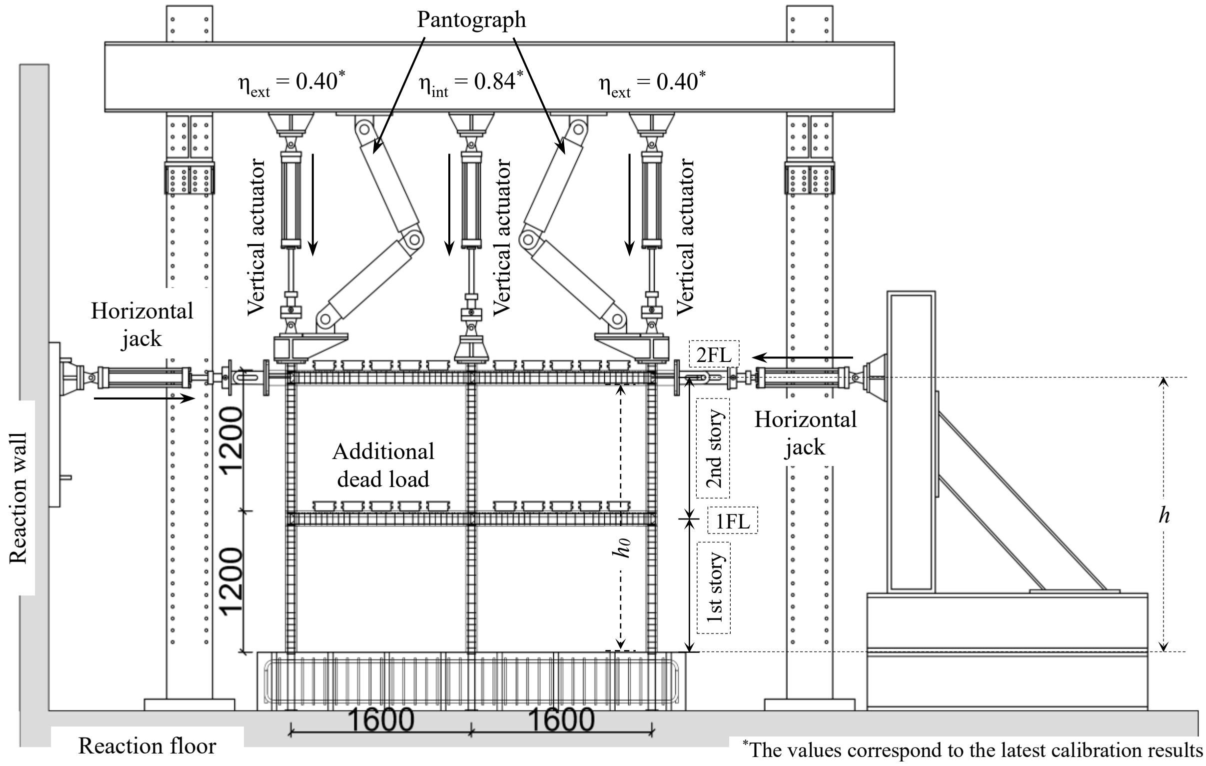

Fig. 6 – Loading system of the experiment

3. Experimental results

3.1 BF specimen

Fig. 7 shows the horizontal load-drift angle relationship obtained from the experiment of the BF specimen. During the test setup of the BF specimen, an accidental axial load was applied to the left exterior loading beam. The lateral positive loading was started in the right-to-left direction to minimize the unfavorable effects on the specimen's behavior.

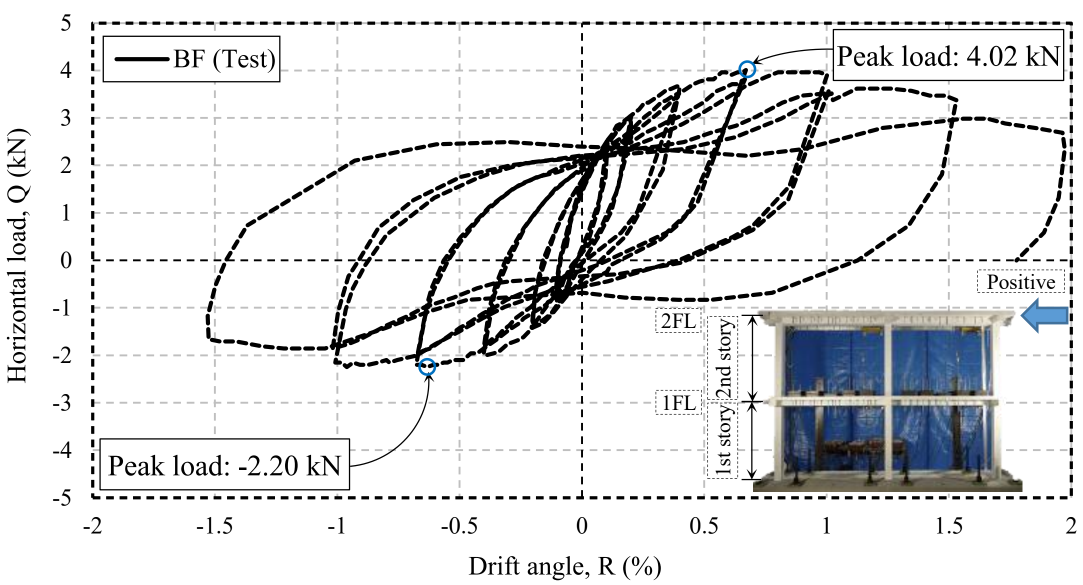

Fig. 7 – Horizontal load-drift angle relationship from the experiment of BF specimen

Flexural cracks were observed at the base of the left side column of the 1st story during the 1st cycle of +0.1% target drift, and at the top of the right-side column of the 1st story during the 2nd cycle of -0.1% target drift. During the ± 0.4% target drift cycle, cracks due to the pullout of longitudinal bars were observed at the bottom of all 1FL (floor level) beam ends. During the ±0.67% target drift cycle, new flexural cracks and the progress of other existing cracks were observed at the column ends. In addition, at the top of the 2nd story interior column, compressive yielding of longitudinal bars due to a combination of bending and the high axial load was observed. The peak lateral load of 4.02kN on the positive side and -2.20kN on the negative side were measured during this loading cycle. The development of new flexural cracks was observed at the ends of all members after the ±1.0% drift cycle. When the lateral load fell below 80% of the maximum lateral load on the 2nd cycle of 1.5% target drift, loading was continued up to 2.00% and terminated afterward.

3.2 BF+MIW specimen

Fig. 8 shows the horizontal load-drift angle relationship obtained from the experiment of the BF+MIW specimen. In the experiment of the BF+MIW specimen, the lateral load direction from left-to-right is considered as positive and vice versa. During the 1st cycle of +0.1% target drift, tensile cracks were observed in the interior column which was at the tension side of the wall. Additionally, vertical cracks were observed at the interface between the interior column and the wall and lateral cracks were observed at the RC beam-wall interface at the bottom of the wall in the 1st story. During the ±0.4% target drift cycle, the tensile cracks of the columns attached to the wall (e.g. interior and left side column) were increased and shear cracks at the top of interior columns of both stories were observed. Additionally, the yielding of longitudinal bars was observed in the tension side columns. The specimen reached the maximum lateral capacity in the 1st cycle of ±0.4% target drift which was +66.20kN and -52.50kN for positive and negative side loading respectively. At the 1st cycle of +0.67% target drift, a distinct failure mode of the tension side column (i.e. the interior column), *column snap-through* shear failure was observed which was simultaneously accompanied by sliding at the beam-wall interface at the top of 1st story wall. During the 1st cycle of -0.67% target drift, sliding failure of the wall accompanied by the pullout of the longitudinal bars of the beams and slabs at the right exterior beam-column joint, and cracking of the wall was observed. The lateral load was then fell below less than 80% of the peak load, hence the loading was terminated after this target drift cycle (as shown by solid lines in Fig. 8). Later, a pushover load was applied to the specimen up to 1.57% drift as shown by the dotted lines in Fig. 8.

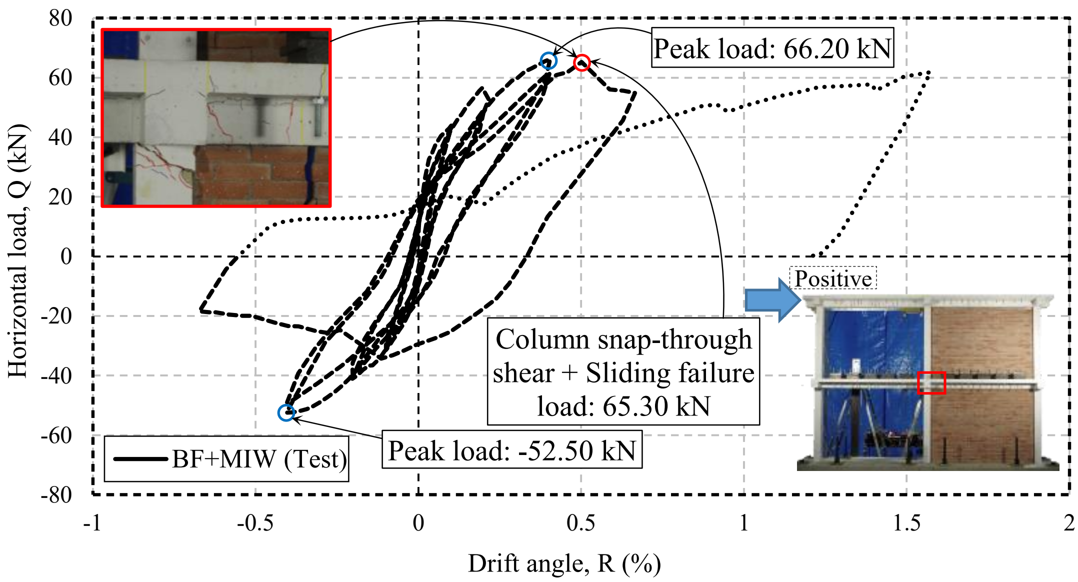

Fig. 8 – Horizontal load-drift angle relationship from the experiment of BF+MIW specimen

4. Failure mechanism and maximum strength evaluation

4.1 BF specimen

Due to the high axial forces applied to the column, the strength degradation of the BF specimen by the P-Δ effect is not negligible and needs to be considered. The red line of Fig. 9 shows the horizontal load-drift angle relationship of the specimen by adding the horizontal component of the forces applied by the axial jacks (i.e. ignoring strength degradation due to P-Δ effect).

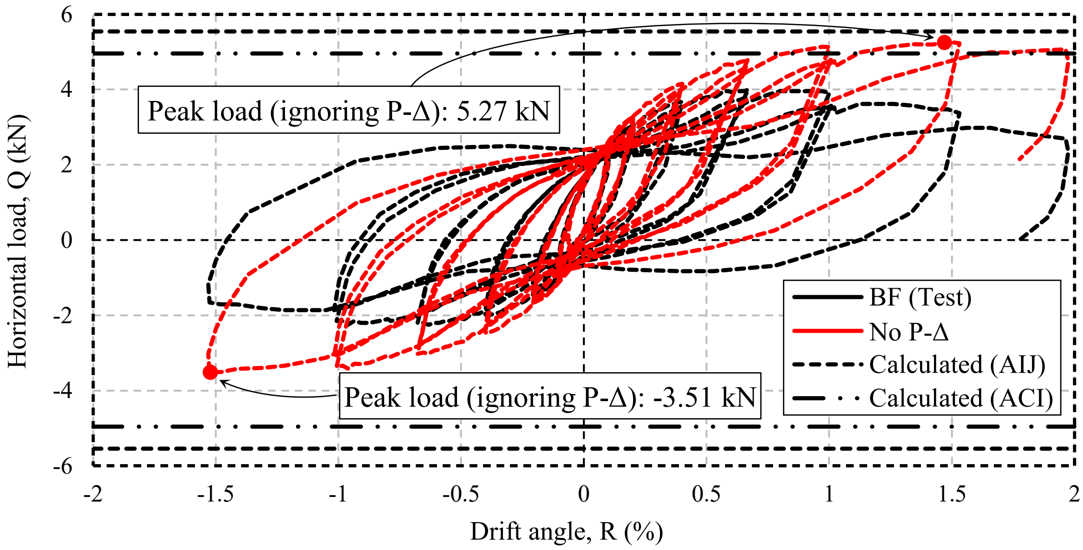

Fig. 9 – Horizontal load-drift angle relationship of the BF specimen by ignoring the P-Δ effect

The failure mechanism of the BF specimen is investigated based on the curvature distribution of columns derived from the obtained strains of column longitudinal bars from the experiment or equilibrium of nodal moment as shown in Fig. 10. Strain gauges at some locations were damaged during the construction of the specimen, as a result, several strain gauge data could not be obtained. These locations are marked by "×" in Fig. 10(a). Even in such cases, the curvature at the end of the member was calculated from the equilibrium of the nodal moments as shown by "▲". Fig. 10(a) demonstrates that the curvatures in the 1st story column bottom and the 2nd story column top show the maximum values for all three columns while they are almost zero on the 1st story beam faces. This result can be attributed to the pull-out failure of beam longitudinal bars. Based on this observation, the moment distribution and the failure mechanism at the maximum load are assumed, as shown in Fig. 10(b). The bending moments at the bottom of the 1st story and the top of the 2nd story for each column reach their ultimate capacity, ${}_cM_u$.

The lateral capacity of the BF specimen, Q_u is then calculated as shown in Table 3, considering the clear height of columns, h_0 = 2270mm as shown in Fig. 6. In the present study, ${}_cM_u$ is calculated using two different methods; (a) the AIJ standard [6] as shown by Eq. (1) and (b) the stress block method [5].

$$
{}_cM_u = \begin{cases} 0.6a_t f_y D + 0.5ND\left(1 - \dfrac{N}{bDf_c'}\right); \textit{ for } 0.4bDf_c' \geq N > 0 \\ 0.6a_t f_y D + 0.5ND\left(\dfrac{N_{max} - N}{N_{max} - 0.4bDf_c'}\right); \textit{ for } N_{max} \geq N > 0.4bDf_c' \end{cases} \tag{1}
$$

Here, ${}_cM_u$ = flexural capacity of an RC column section; b = width of member cross-section; D = depth of member cross-section; a_t = total cross-sectional area of the tensile reinforcing bars in the RC section; f_y =

yield strength of longitudinal bars; N = applied axial load to the section; f_c' = compressive strength of concrete; N_{max} = axial compressive capacity of the RC member section. In the Eq. (1), the factor of 0.6 is used instead of 0.8 of the original equation, considering the small ratio of the "distance of longitudinal bars from the compressive fiber" to the column depth, D. However, the calculated values are slightly higher than the average of the peak horizontal loads, 4.39kN obtained from the experiment.

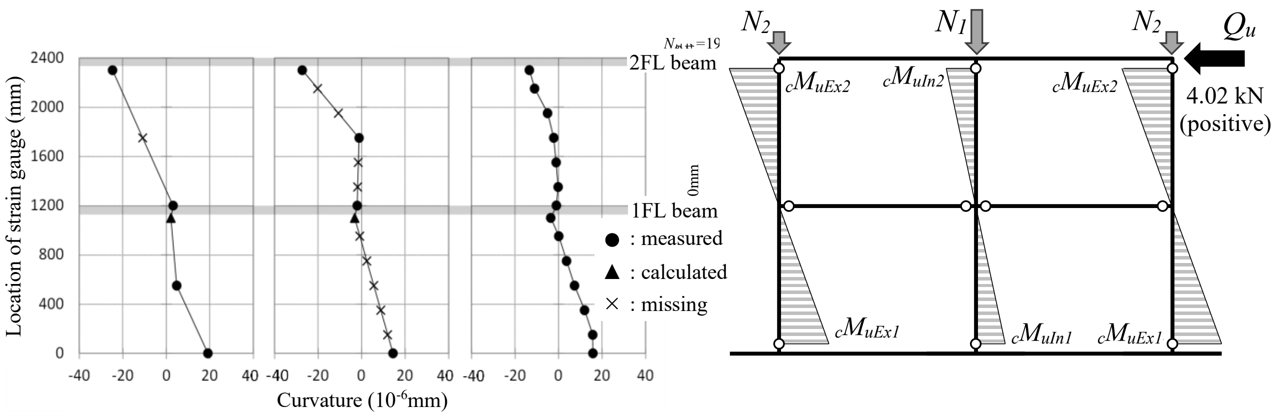

(a) curvature distribution (b) assumed moment distribution

Fig. 10 – Assumption of moment distribution based on obtained curvature from the experiment of BF specimen; (a) curvature distribution from the strain gauge measurements; (b) assumed moment distribution

Table 3 – Maximum lateral strength calculation for BF specimen

Calculation method	Members	Location	$_cM_u$ (kN-m)	h_0 (mm)	Shear force at $_cM_u$, Q_{cmu} (kN)	Q_u (kN)
AIJ	Interior column	2nd story top	2.59	2270	1.92	5.54
		1st story bottom	1.77			
	Exterior column	2nd story top	2.14		1.81	
		1st story bottom	1.98			
ACI stress block	Interior column	2nd story top	2.00		1.50	4.96
		1st story bottom	1.41			
	Exterior column	2nd story top	2.05		1.73	
		1st story bottom	1.70			

4.2 BF+MIW specimen

During the positive loadings, all longitudinal bars of the interior column (acting as tension column in this context) yielded at its bottom section and large horizontal cracks appeared at the bottom of the wall due to the bending moment there. In contrast, during the negative loadings, similar behavior was observed in the right exterior column (acting as tension column in this context) and the wall. Therefore, as shown in Fig. 11(a), the wall and boundary columns are assumed to be acting as a cantilever member. The maximum strength of this cantilever member, Q_{WMU} is calculated from the mechanism of forces when all rebars in tensile column yields as shown in Fig. 11(a). From the equilibrium of moments, Q_{WMU} is calculated by Eq. (2).

$$Q_{WMU} \cdot h - N_l \cdot l_c - T_y \cdot l_c = 0 \tag{2}$$

Here, h = distance from the base to 2FL beam center, N_I = applied axial load in the interior column; l_c = distance between interior and right exterior column center; T_y = axial tensile capacity of the column. The left column shear force Q_{cmu} is calculated by the ACI stress block method [5] under the assumptions explained in section 4.1.

The assumed mechanism of forces at the simultaneous *column snap-through* shear failure and sliding at the beam-wall interface as shown in Fig. 11(b), the shear strength of this failure mode, Q_U' is calculated as the sum of the *column snap-through* shear strength of the 1st story interior column top ${}_PQ_C$, the sliding shear strength at the beam-wall interface Q_{sl}, and the shear force of the 1st story right exterior column in compression, Q_{C2}.

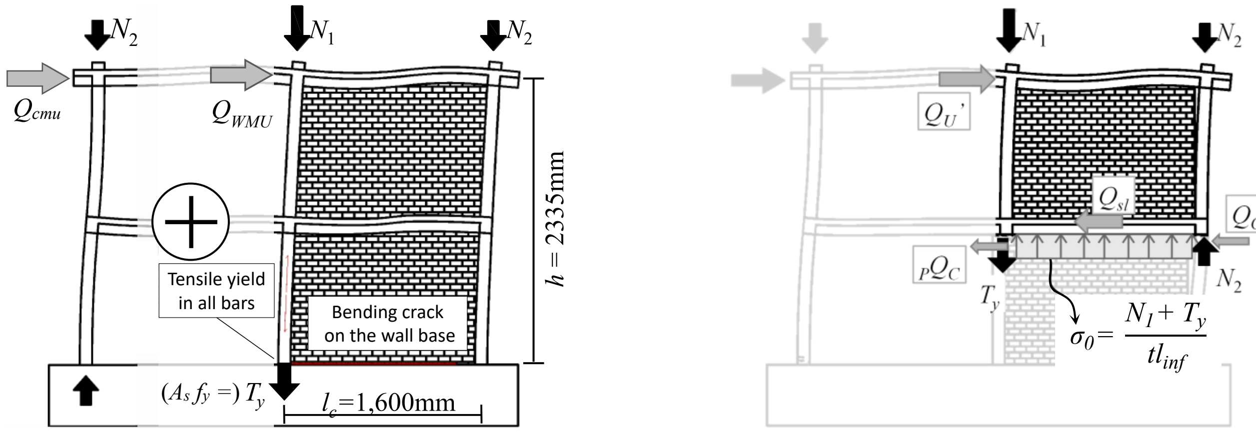

(a) at peak lateral capacity

(b) *column snap-through* shear failure and simultaneous sliding at the beam-wall interface

Fig. 11 – Assumed load resistance mechanism of the BF+MIW specimen; (a) at peak lateral capacity; (b) *column snap-through* shear failure and simultaneous sliding at the beam-wall interface

According to FEMA 306 [11] *column snap-through* shear failure occurs if the infill is relatively stiffer and stronger than the surrounding frame and the shear cracks in a column in this context do not appear across a corner to corner diagonally, and rather they appear in a flatter angle and the shear cracks in the column remain within a length of two-member widths (i.e. $\leq 2D$) which is a very severe case. The *column snap-through* shear strength, ${}_PQ_C$ is calculated by using Eqs. (3) – (6) as suggested by the standard of the JBDPA [7].

$${}_pV_c = K_{min}\,\tau\,A_c \tag{3}$$

$$K_{min} = \frac{0.34}{0.52 + a/D} \tag{4}$$

$$\tau = \begin{cases} 0.98 + 0.1f_c' + 0.85\sigma; & if,\ 0 \leq \sigma \leq 0.33f_c' - 2.75 \\ 0.22f_c' + 0.49\sigma; & if,\ 0.33f_c' - 2.75 \leq \sigma \leq 0.66f_c' \end{cases} \tag{5}$$

$$\sigma = (A_s f_y)/(A_c) + \sigma_{c0} \tag{6}$$

Here, A_c = cross-sectional area of the column; A_s = area of all longitudinal bars in the column; σ_{c0} = axial stress on the column acting at the collapse point. It is assumed for Fig. 11(b) that the interior column is in tension. This condition reduces the *snap-through* shear strength of the column. In this case, σ_{c0} can be determined by using Eq. (7) by conservatively assuming that the interior column is at its tensile capacity i.e., the longitudinal bars have been yielded. The negative sign of Eq. (7) is for axial force in tension. This makes the value of σ in Eq. (6) to be 0.

$$\sigma_{co} = - \left(A_s f_y \right) / \left(A_c \right) \tag{7}$$

As for the BF+MIW specimen, $0.33f_c^{'}$-$2.75 \leq \sigma \leq 0$, hence the value of τ is taken as the minimum of the two values obtained from Eq. (5). The shear span, a is taken as $0.5D$ based on experimental observation ($a \leq D$).

The sliding shear strength at the beam-wall interface, Q_{sl} is evaluated by using Eq. (8) based on the Mohr-Coulomb failure criterion. It is assumed that (1) an uniformly distributed normal stress, σ_0 is acting over the cross-section of the wall at the beam-infill interface, which can be determined by using Eq. (9), considering the mechanism of forces acting on the frame as shown in Fig. 11(b). It is also assumed that (2) all the longitudinal bars of the interior column are yielded since the column rebars yielded over the entire height of the 1st story interior column during the test and (3) the reaction force on the right exterior column is generated by the applied axial load N_2.

$$Q_{sl} = (\tau_s + \mu\sigma_0)\, tl_{inf} \tag{8}$$

$$\sigma_0 = \frac{N_1 + T_y}{tl_{inf}} \tag{9}$$

Here, t = thickness of the wall; l_{inf} = width of the wall; N_1 = axial force on the interior column. Walls are generally constructed after the construction of the frame structure. Inserting mortar between the infill and the upper beam is inconvenient and depends on the quality of the workmanship. Moreover, the bed mortar bond at the beam-infill interface might be broken at the initial stages of lateral loading. Thus, the bed mortar shear strength, τ_s (i.e. cohesion of mortar) can be ignored while evaluating Q_{sl} using the Mohr-Coulomb failure criterion. The value of the coefficient of friction, μ is taken as 0.58 [12]. Q_{C2} is then calculated as the shear force assuming yield hinge formation at both ends of the 1st story right exterior column. The calculated results for the BF+MIW specimen are shown in Table 4, which shows good agreement with the experimental results with some underestimation.

Table 4 – Comparison of test results and calculated results

Direction	Peak lateral capacity				Simultaneous *column snap-through* shear failure and sliding at beam-wall interface				
	Q_{WMU} (kN)	Q_{cmu} (kN)	$Q_{WMU} + Q_{cmu}$ (kN)	Test results $\lvert Q\rvert_{max,test}$ (kN)	${}_{P}Q_C$	Q_{sl}	Q_{C2}	$Q_U{}'$	Test results $\lvert Q\rvert_{U,\ test}$ (kN)
Positive	62.73	1.65	64.38	66.20	3.83	53.10	3.27	60.20	65.30
Negative	47.06		48.71	52.50					

5. Conclusion

The current study presents an experimental study of two 1/2.5 scale 2-story 2-bay RC frames with low strength concrete and straight anchorage under high axial loads and cyclic static lateral loading simulating the behavior of inappropriately designed existing buildings in Bangladesh. To investigate the effect of masonry infill walls on the seismic performance of RC frames, MIWs were added to the right bay of both stories of the BF+MIW specimen. The failure mechanism of both RC frames is investigated, and their maximum lateral capacities are evaluated and compared with experimental results.

Pullout failure of the beam longitudinal bars at the 1FL exterior beam-column joints of the BF specimen was observed in the experiment. Yielding column longitudinal bars were observed at the bottom of 1st story columns and at the top of 2nd story columns. The lateral capacity of the BF specimen was evaluated using the ACI stress block method and AIJ standard based on the failure mechanism presented in Fig. 10. Both methods showed slightly overestimated and similar results. However, the ACI stress block method showed relatively better accuracy.

The peak lateral strength of the BF+MIW specimen was approximately more than 10 times higher than the BF specimen. A distinct failure mode, *column snap-through* shear failure was observed in the interior column of the BF+MIW specimen. This failure was simultaneously accompanied by sliding failure at the beam-wall interface of the 1st story. The *column snap-through* shear strength and sliding at the beam-wall interface were evaluated using JBDPA standard and Mohr-Coulomb failure criterion respectively. The estimated results for the BF+MIW showed good agreement with the experimental results with some underestimation.

Acknowledgments This study is supported by the JICA/JST **S**cience **a**nd **T**echnology **Re**search **P**artnership for **S**ustainable Development–project for **T**echnical Development to Upgrade **S**tructural Integrity of Buildings in Densely Populated **U**rban Areas and Its Strategic **I**mplementation towards Resilient Cities in **B**angladesh (SATREPS–TSUIB), directed by Mohammad Shamim Akhter (Housing and Building Research Institute, Bangladesh) and Prof. Yoshiaki Nakano (The University of Tokyo, Japan) and it is gratefully acknowledged.

6. References

[1] Japan International Cooperation Agency, OYO International Corporation, Mohri Architect & Associates Inc. (2015): Project for Capacity Development on Natural Disaster-Resistant Techniques of Construction and Retrofitting for Public Buildings in The People's Republic of Bangladesh Final Report.

[2] Japan International Cooperation Agency, OYO International Corporation, Mohri Architect & Associates Inc. (2015): Data Collection Survey on Urban Building Safety in the People's Republic of Bangladesh.

[3] PWD (2015): *Manual for Seismic Evaluation of Existing Reinforced Concrete Buildings*. Public Works Department, The People's Republic of Bangladesh.

[4] BNBC (1993): *Bangladesh National Building Code*. Housing and Building Research Institute and Bangladesh Standards and Testing Institution.

[5] ACI Committee 318 (2011): *Building Code Requirements for Structural Concrete (ACI 318M-11) and Commentary*. Farmington Hills, MI: American Concrete Institute.

[6] AIJ (2010): *AIJ standard for structural calculation of reinforced concrete structures (in Japanese)*. Architectural Institute of Japan, Tokyo.

[7] JBDPA (2016): *Standard for seismic evaluation of existing reinforced concrete buildings (in Japanese)*. Japan Building Disaster Prevention Association, Tokyo, Japan.

[8] Fukutomi Y (2019): Experimental study of vulnerable RC frames with unreinforced masonry infill wall (in Japanese). Master's dissertation, Graduate School of Engineering, The University of Tokyo.

[9] Adnan SMN, Fukutomi Y, Haga Y, Matsukawa K, Nakano Y (2019): Experimental study of vulnerable RC frames with unreinforced masonry infill wall Part 1: Test Program and Results. *Annual Meeting of the Architectural Institute of Japan*. Architectural Institue of Japan (AIJ), Kanazawa, 617–618.

[10] Fukutomi Y, Haga Y, Matsukawa K, Nakano Y (2019): Experimental study of vulnerable RC frames with unreinforced masonry infill wall Part 2: Maximum strength evaluation. *Annual Meeting of the Architectural Institute of Japan*. Architectural Institue of Japan (AIJ), Kanazawa, 619–629.

[11] FEMA 306 (1998): *Evaluation of earthquake damaged concrete and masonry wall buildings: Basic procedures manual*. ATC, Redwood City, CA, USA.

[12] Sanada Y, Nakamura Y, Yamauchi N, Choi H, Nakano Y (2006): A method to enhance seismic performances of unreinforced masonry structures derived from lateral force resisting mechanisms of masonry infilled frames (in Japanese). *Journal of Structural and Construction Engineering (Transactions of AIJ)*, **605**, 159–166.

